

Infrared spectrum of the  $\text{NH}_4\text{-}d_n^+$  cation trapped in solid neon

Marilyn E. Jacox\* and Warren E. Thompson†

*Optical Technology Division, National Institute of Standards and Technology‡, Gaithersburg, MD 20899-8441, USA. E-mail: marilyn.jacox@nist.gov**Received 21st September 2004, Accepted 17th November 2004  
First published as an Advance Article on the web 17th December 2004*

The  $\text{NH}_4^+$  cation has been stabilized in solid neon in sufficient concentration for the identification of both of its infrared-active vibrational fundamentals, which appear within a few wavenumbers of the gas-phase band centers. Systematic alteration of the concentrations and positions of introduction of  $\text{NH}_3$  and  $\text{H}_2$  in the discharge sampling experiments demonstrated that the highest yield of  $\text{NH}_4^+$  resulted when both the  $\text{NH}_3$  and the  $\text{H}_2$  were introduced downstream from a discharge through pure neon. In this configuration, each of these molecules can be ionized by excited neon atoms and their resonance radiation (16.6 eV to 16.85 eV), but fragmentation is minimized. Both infrared-active vibrational fundamentals of  $\text{ND}_4^+$  and several fundamentals of each of the partially deuterium-substituted isotopomers of  $\text{NH}_4^+$  were also identified. Evidence is presented for complexation of  $\text{NH}_4^+$  with an H atom or with one or more  $\text{H}_2$  molecules.

## I. Introduction

Because of the chemical and biological importance of the ammonium cation,  $\text{NH}_4^+$ , there have been many observations of its infrared absorption spectrum in the strongly interacting environments of ionic crystals and polar solvents. In contrast, studies of its spectroscopic behavior in the absence of these interactions are sparse. The first gas-phase observations of  $\text{NH}_4^+$  were concurrent studies by Crofton and co-workers<sup>1,2</sup> and by Schäfer and co-workers,<sup>3,4</sup> which yielded the assignment of the infrared-active stretching fundamental,  $\nu_3$ . The other infrared-active fundamental of gas-phase  $\text{NH}_4^+$ ,  $\nu_4$ , was later observed in diode laser studies.<sup>5,6</sup> Crofton and co-workers<sup>2</sup> also analyzed the  $\nu_3$  band of  $\text{ND}_4^+$ , and, in a study of the zero-kinetic-energy photoelectron spectrum of  $\text{ND}_4$ , Signorell and co-workers<sup>7</sup> obtained the rotational constant of ground-state  $\text{ND}_4^+$  with an uncertainty of  $0.004\text{ cm}^{-1}$ . Except for the analysis of one vibrational fundamental of  $\text{NH}_3\text{D}^+$  by Nakagawa and Amano,<sup>8</sup> there have been no experimental studies of the partially deuterium-substituted ammonium cations. The CCSD(T)/cc-pVTZ *ab initio* calculations, including anharmonic corrections, by Martin and Lee<sup>9</sup> of the vibrational fundamentals of  $\text{NH}_4^+$  and all of its deuterium-substituted isotopomers provide tentative information regarding the spectroscopic properties of these species.

Experiments in this laboratory have led to the stabilization of a number of small molecular ions in concentration sufficient for infrared identification.<sup>10</sup> In the study of the infrared spectrum of  $\text{NH}_3^+$ ,<sup>11</sup> a weak absorption appeared near the position of the  $\nu_4$  fundamental of gas-phase  $\text{NH}_4^+$ ,  $1447.22\text{ cm}^{-1}$ .<sup>5,6</sup> In order to determine whether this peak was indeed contributed by  $\text{NH}_4^+$  and, if so, to optimize the conditions for  $\text{NH}_4^+$  production, further studies were conducted using several different sampling configurations and introducing additional  $\text{H}_2$  into the system. As will be shown in the following discussion, not only did these studies confirm the identification of  $\text{NH}_4^+$ , but they yielded the first spectroscopic identification of  $\nu_4$  of  $\text{ND}_4^+$  and of many of the vibrational fundamentals of the partially deuterium-substituted isotopomers.

II. Experimental details<sup>12</sup>

The ammonia samples used for these studies were the same as had been used for the previous series of experiments<sup>11</sup> concerned with the identification of isotopomers of  $\text{NH}_3^+$ . These samples were freed of relatively volatile impurities by freezing at 77 K and pumping on the resulting solid. The  $\text{H}_2$  and  $\text{D}_2$  (Matheson Gas Products, Inc.), HD (97%, Cambridge Isotope Laboratories, Inc.), and neon (Spectra Gases, Inc., Research Grade, 99.999%) were used without further purification. Sample mixtures were prepared using standard vacuum procedures. A number of initial experiments were conducted in order to establish optimal conditions for the stabilization of  $\text{NH}_4^+$  and its isotopomers. For these studies, the concentrations of the reactants were varied. The concentrations which will be given in the description of the initial experiments were representative. The optimum Ne :  $\text{H}_2$  :  $\text{NH}_3$  mole ratio was found to be 400 : 6 : 1. After this had been established, more detailed isotopic substitution studies were conducted at a Ne :  $\text{H}_2\text{-}d_m$  :  $\text{NH}_3\text{-}d_n$  mole ratio of 400 : 6 : 1 or 400 : 5 : 1.

Isotopically enriched ammonia undergoes significant isotopic exchange with ammonia which has previously been adsorbed on the walls of deposition line. The extent of isotopic enrichment improved as a series of experiments on a given isotopically enriched sample proceeded. Flowing some of the sample mixture through the deposition system and cell before the cell was cooled for the experiment enhanced the extent of isotopic enrichment.

A Helitran (APD Cryogenics, Inc.) continuous transfer liquid helium cell maintained at 4.3 K was used for all of the experiments. The deposition configuration has previously been described,<sup>13</sup> as has been the setup used for microwave excitation.<sup>14</sup> In typical ion production experiments, pure neon is subjected to a microwave discharge while it passes through a quartz tube that has a coarse pinhole in the end. The molecule of interest, mixed with a large excess of neon, is introduced into the cell slightly beyond the discharge tube, and the excited neon atoms and their resonance radiation interact with the molecule outside the pinhole and on the cryogenic surface. In some of the preliminary experiments, the two deposition lines were interchanged, so that the ammonia-containing mixture passed through the microwave discharge and additional neon was introduced into the sample without exposure to the discharge.

† Guest researcher, National Institute of Standards and Technology.

‡ Technology Administration, US Department of Commerce.

In a few experiments, a small concentration of  $H_2$  was added to the neon sample flowing through the discharge tube.

The absorption spectra of the sample deposits were obtained using a Bomem DA3.002 Fourier transform interferometer with transfer optics that have been described previously.<sup>15</sup> Observations were conducted with a resolution of  $0.2\text{ cm}^{-1}$  between 400 and  $5000\text{ cm}^{-1}$  using a globar source, a KBr beamsplitter, and a wide-band HgCdTe detector cooled to 77 K. Data were accumulated for each spectrum over a period of at least 15 min. The resulting spectrum was ratioed against a similar one taken without a deposit on the cryogenic mirror. Under these conditions, the positions of the prominent, non-blended atmospheric water vapor lines between  $1385$  and  $1900\text{ cm}^{-1}$  and between  $3620$  and  $3900\text{ cm}^{-1}$ , observed in a calibration scan, agreed to within  $0.01\text{ cm}^{-1}$  with the high-resolution values reported by Toth.<sup>16,17</sup> Based on previous investigations, with this experimental configuration the standard uncertainty (type B) in the determination of the positions of absorption maxima for molecules trapped in solid neon is  $\pm 0.1\text{ cm}^{-1}$  (coverage factor,  $k = 1$ , i.e.,  $1\sigma$ ).

Information on photoinduced changes in the matrix sample was obtained by exposing the deposit to various wavelength ranges of visible and ultraviolet radiation. For a few studies, a tungsten background source was used with a 780 nm (Schott glass type RG780) or a 630 nm (Corning glass type 2403) short-wavelength cutoff filter. Since no changes were detected in the product spectra under those irradiation conditions, most of the sample irradiations were conducted using a medium-pressure mercury arc with a filter of Corning glass type 3384, 3389 or 7740 or without a filter to provide a short-wavelength cutoff of approximately 490, 420, 280 or 250 nm, respectively.

### III. Results and discussion

#### A. Stabilization of $NH_4^+$

The initial experiments were focused on determining the conditions that produce the greatest intensity of the product absorption which was previously detected<sup>11</sup> at  $1442.5\text{ cm}^{-1}$  when a Ne :  $NH_3$  sample was codeposited with a beam of discharged neon atoms. The results of these experiments are summarized in Fig. 1. The initial strategy was to pass the Ne :  $NH_3$  mixture, rather than pure neon, through the microwave discharge and, to improve the isolation of the products in the solid deposit, diluting the discharged material with an approximately equal amount of pure neon that had not been excited in the discharge. Similar conditions have been used in many laboratories to produce molecular fragments for spectroscopic study. As is shown in trace (a), a weak absorption at  $1442.5\text{ cm}^{-1}$  resulted. When a mixture with a greater concentration of  $NH_3$  was used, as in trace (b), a somewhat more intense product absorption appeared. Since the isolation properties of the neon matrix would be likely to degrade at still higher concentrations of  $NH_3$ , the introduction of  $H_2$  was next tried. The first such study, shown in trace (c), involved passing a Ne :  $H_2$  :  $NH_3 = 400 : 4 : 1$  mixture through the microwave discharge. Further enhancement of the  $1442.5\text{ cm}^{-1}$  absorption resulted. When, as in trace (d), a still higher concentration of  $H_2$  was present in the sample mixture, the  $1442.5\text{ cm}^{-1}$  peak and satellite absorptions at  $1441.2$  and  $1440.9\text{ cm}^{-1}$  grew still more. In the experiments of traces (b) through (d), a new absorption at  $3357.5\text{ cm}^{-1}$  appeared and grew in prominence. It was not feasible to increase the  $H_2$  concentration in the mixture passed through the discharge tube beyond about 2.5%, the value employed for the experiment of trace (d); at higher concentrations spontaneous warmups of the deposit frequently occurred. The experiment of trace (e) more closely followed the procedure which has typically been used for ion production studies in this laboratory. The Ne :  $NH_3$  mixture was introduced into the system downstream from the discharge

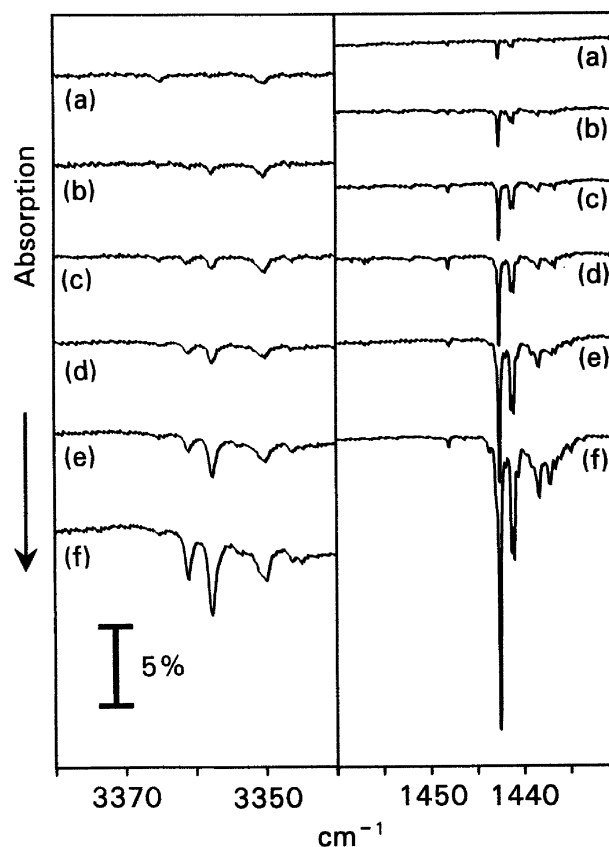


**Fig. 1** (a) 10.7 mmol Ne :  $NH_3 = 400 : 1$  that had been passed through a microwave discharge was codeposited at 4.3 K over a period of 205 min with 10.9 mmol undischarged Ne. (b) 9.04 mmol Ne :  $NH_3 = 200 : 1$  that had been passed through a microwave discharge was codeposited at 4.3 K over a period of 180 min with 8.19 mmol undischarged Ne. (c) 9.17 mmol Ne :  $H_2$  :  $NH_3 = 400 : 4 : 1$  that had been passed through a microwave discharge was codeposited at 4.3 K over a period of 181 min with 9.23 mmol undischarged Ne. (d) 9.21 mmol Ne :  $H_2$  :  $NH_3 = 400 : 10 : 1$  that had been passed through a microwave discharge was codeposited at 4.3 K over a period of 180 min with 9.31 mmol undischarged Ne. (e) 7.20 mmol undischarged Ne :  $NH_3 = 400 : 1$  was codeposited at 4.3 K over a period of 140 min with 6.68 mmol Ne :  $H_2 = 39 : 1$  that had been passed through a microwave discharge. (f) 9.77 mmol undischarged Ne :  $H_2$  :  $NH_3 = 400 : 6 : 1$  was codeposited at 4.3 K over a period of 231 min with 9.96 mmol Ne that had been passed through a microwave discharge.

region. A Ne :  $H_2 = 39$  mixture was passed through the microwave discharge, providing a source not only of excited neon atoms and their resonance radiation but also of H atoms and undissociated  $H_2$ . Although care had been taken to match the sample size and deposition time in the other experiments in this comparison, only a limited amount of liquid helium was available to conduct the experiment shown in trace (e). Despite the smaller sample size, both the absorption pattern near  $1442.5\text{ cm}^{-1}$  and that near  $3357.5\text{ cm}^{-1}$  were more prominent than in the earlier studies. Finally, an experiment was conducted using an undischarged Ne :  $H_2$  :  $NH_3 = 400 : 6 : 1$  sample mixture and passing pure neon through the microwave discharge. As is shown in trace (f) of Fig. 1, the absorptions of interest were approximately doubled in intensity, compared to those of trace (e). Subsequent experiments were conducted using the same sampling configuration and approximately the same concentrations in the sample mixture as had been used for the experiment of trace (f).

The assignment of the absorption at  $1442.5\text{ cm}^{-1}$  to the  $\nu_4$  fundamental of  $NH_4^+$  is supported not only by its proximity to the gas-phase band center of that species but also by the enhancement in its intensity as hydrogen is added to the system. The absorption at  $3357.5\text{ cm}^{-1}$  and a less intense absorption at  $3361.0\text{ cm}^{-1}$  that grow at a rate proportional

to that of the structured  $1442.5\text{ cm}^{-1}$  absorption in the experiments summarized by Fig. 1 lie suitably close to the  $3343.14\text{ cm}^{-1}$  gas-phase band center<sup>1–4</sup> of  $\nu_3$  of  $\text{NH}_4^+$  for the corresponding assignment. A series of molecular beam studies by Dopfer, Maier and co-workers, recently reviewed by Bieske and Dopfer,<sup>18</sup> have shown that the H-stretching vibrational band centers of complexes of the rare gases with protonated molecules are often shifted to appreciably lower frequencies because of proton sharing with the rare gas atom. However, the proton affinity of  $\text{NH}_3$  is relatively high, and the  $\nu_3$  band center of gas-phase  $\text{NH}_4^+$  complexed to a single neon atom appears at  $3344.0\text{ cm}^{-1}$ ,<sup>19</sup> very close to the band center for the uncomplexed cation.

When both  $\text{NH}_3$  and  $\text{H}_2$  are present in the sample deposit, the detailed structure of the infrared absorptions of the  $\text{NH}_3$  differs from that characteristic of simple  $\text{Ne} : \text{NH}_3$  deposits.<sup>20,21</sup> This phenomenon is attributed to complex formation between  $\text{H}_2$  and  $\text{NH}_3$ , previously reported by Moroz and co-workers.<sup>22</sup> Further discussion of perturbations to the spectrum of  $\text{NH}_3$  is beyond the scope of the present study.

In the experiment of Fig. 1(f), as well as in the other experiments here reported, the presence of  $\text{H}_2$  or its isotopomers greatly inhibits the stabilization of  $\text{NH}_3^+$  or its isotopomers.

All of the absorptions shown in Fig. 1 except that of  $\text{NH}_3$  at  $3350\text{ cm}^{-1}$  were somewhat diminished in intensity when the sample was exposed for a few minutes to mercury-arc radiation of wavelength longer than  $490\text{ nm}$  and were destroyed when a  $420\text{ nm}$  cutoff filter was instead used or the filter was removed during the irradiation. The absorptions of ammonia showed little or no change as a result of this irradiation.

## B. Isotopic dependence of the $\text{NH}_4^+$ absorptions

Still further support for the assignment of the  $1442.5$  and  $3357.5\text{ cm}^{-1}$  neon-matrix absorptions to the two infrared-active vibrational fundamentals of  $\text{NH}_4^+$  has been obtained

from experiments on isotopically substituted samples. In addition, these experiments have yielded the first infrared spectroscopic data for several isotopomers of  $\text{NH}_4^+$ .

As is shown in Table 1, the  $1442.5$  and  $3357.5\text{ cm}^{-1}$  neon-matrix absorptions also agree well with the positions obtained for these two vibrational fundamentals of  $\text{NH}_4^+$  in the CCSD(T)/cc-pVTZ calculations including anharmonic corrections by Martin and Lee.<sup>9</sup> Although these workers obtained vibrational fundamental frequencies for all of the  $^{14}\text{NH}_4-d_n^+$  species, estimates of their relative intensities were not reported. Since these would also be helpful in the assignments and since some of the experiments were conducted using ammonia samples which were enriched in nitrogen-15, we performed calculations for the various isotopomers of the ammonium cation at the RMP2/6-311++G(3df,3pd) level using the Gaussian 98 program package.<sup>23</sup> The intensities estimated for the vibrational fundamentals of the  $^{14}\text{NH}_4-d_n^+$  species by these calculations are included, in parentheses, in Table 1. Assignments of observed absorptions are also summarized. The observations leading to these assignments are described in the following discussion.

$\text{NH}_3\text{D}^+$  should have two relatively prominent deformation fundamentals, one only slightly shifted from the triply degenerate deformation fundamental of  $\text{NH}_4^+$ , the other near  $1278.6\text{ cm}^{-1}$ . The latter spectral region is shown in Fig. 2. As is shown in trace (a), from the same experiment on a  $\text{Ne} : \text{H}_2 : \text{NH}_3$  sample as that illustrated in Fig. 1(f), when the sample was not enriched with deuterium no absorption appeared between  $1265$  and  $1280\text{ cm}^{-1}$ . In another experiment in which HD was substituted for  $\text{H}_2$ , shown in trace (b) of Fig. 2, a weak, photosensitive new absorption appeared at  $1277.3\text{ cm}^{-1}$ . The absorption pattern near  $1442.5\text{ cm}^{-1}$  was unchanged from that obtained using  $\text{H}_2$ . In the NH-stretching region, a photosensitive absorption with a high frequency shoulder appeared at  $3353.7\text{ cm}^{-1}$ . In still another experiment using  $\text{D}_2$  instead of  $\text{H}_2$ , shown in Fig. 2(c), the  $1277.3\text{ cm}^{-1}$  absorption appeared with slightly lower intensity and was accompanied by several

**Table 1** Calculated<sup>a</sup> vibrational fundamentals ( $\text{cm}^{-1}$ ) of  $^{14}\text{NH}_4^+-d_n$  compared with absorptions observed<sup>b</sup> in neon-matrix experiments

	$\text{NH}_4^+$	$\text{NH}_3\text{D}^+$	$\text{NH}_2\text{D}_2^+$	$\text{NHD}_3^+$	$\text{ND}_4^+$
Calculated	3345.1(581)	3336.6(390)	3333.4(196)	3311.4(156)	2492.0(300)
Observed	3357.5	3354.2	3350.0		2502.1
Calculated			3297.9(110)	2479.2(200)	
Observed			3306.4		
Calculated		3279.7(58)	2461.8(100)		
Calculated	3236.6(0)	2430.8(65)	2393.5(38)	2370.5(17)	2325.9(0)
Calculated	1690.1(0)	1624.2(50)	1583.7(52)	1426.9(80)	1205.8(0)
Observed				1425.0	
Calculated			1469.2(0)		
Calculated	1447.2(417)	1442.4(136)	1363.5(114)	1140.6(84)	1094.9(153)
Observed	1442.5		1365.9	1139.9	1092.0
Calculated		1278.6(160)	1198.7(73)		
Observed		1277.3			
Calculated			1136.1(42)	1101.0(52)	
Observed				1103.4	

<sup>a</sup> Positions of fundamentals from CCSD(T)/cc-pVTZ calculations, with anharmonic correction, reported by Martin and Lee.<sup>9</sup> Intensities (km/mol), in parentheses, were estimated from RMP2/6-311++G(3df,3pd) calculations performed as a part of the present study. A blank space for a calculated fundamental indicates that it is degenerate with the fundamental above it. <sup>b</sup> Ne matrix, this work. Based on previous investigations, the standard uncertainty (Type B) in the frequency measurement is  $\pm 0.1\text{ cm}^{-1}$  (coverage factor,  $k = 1$ ; i.e.,  $1\sigma$ ). Where the absorption is structured, the position of the most prominent peak is given.

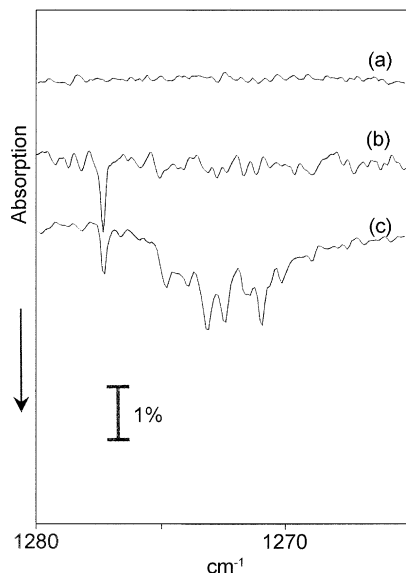


**Fig. 2** (a) 9.77 mmol undischarged Ne : H<sub>2</sub> : NH<sub>3</sub> = 400 : 6 : 1 was codeposited at 4.3 K over a period of 231 min with 9.96 mmol Ne that had been passed through a microwave discharge. (b) 11.1 mmol undischarged Ne : HD : NH<sub>3</sub> = 400 : 6 : 1 was codeposited at 4.3 K over a period of 228 min with 11.4 mmol Ne that had been passed through a microwave discharge. (c) 9.74 mmol undischarged Ne : D<sub>2</sub> : NH<sub>3</sub> = 400 : 6 : 1 was codeposited at 4.3 K over a period of 184 min with 8.01 mmol Ne that had been passed through a microwave discharge.

photosensitive lower frequency absorptions, the most prominent of them at 1274.8, 1273.1, 1272.4 and 1270.9 cm<sup>-1</sup>.

Because of the facile isotopic exchange of ND<sub>3</sub> in the vacuum system, spectra obtained in experiments with more extensive deuterium enrichment are quite complicated. Various spectral regions in which most of the product absorptions appear are shown in Figs. 3–8. Each of these figures shows the results from the same set of four experiments, arranged in

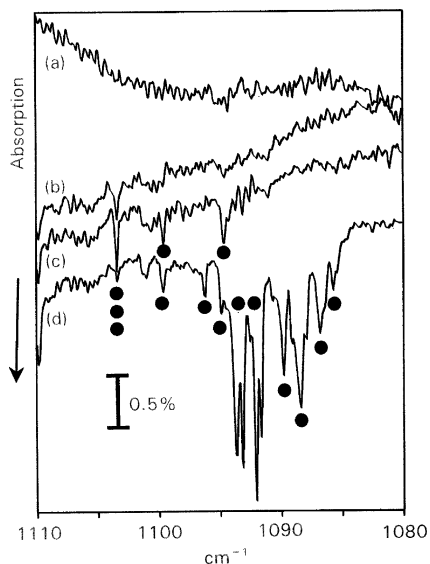


**Fig. 3** (a) 9.77 mmol undischarged Ne : H<sub>2</sub> : NH<sub>3</sub> = 400 : 6 : 1 was codeposited at 4.3 K over a period of 231 min with 9.96 mmol Ne that had been passed through a microwave discharge. (b) 13.4 mmol undischarged Ne : H<sub>2</sub> : ND<sub>3</sub> : NH<sub>3</sub> = 400 : 5 : 0.7 : 0.3 was codeposited at 4.3 K over a period of 250 min with 11.1 mmol Ne that had been passed through a microwave discharge. (c) 11.8 mmol undischarged Ne : H<sub>2</sub> : ND<sub>3</sub> = 400 : 5 : 1 was codeposited at 4.3 K over a period of 220 min with 9.63 mmol Ne that had been passed through a microwave discharge. (d) 11.4 mmol undischarged Ne : D<sub>2</sub> : ND<sub>3</sub> = 400 : 5 : 1 was codeposited at 4.3 K over a period of 215 min with 9.30 mmol Ne that had been passed through a microwave discharge.

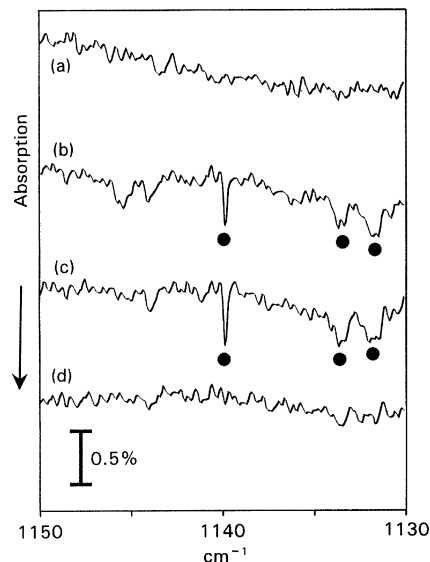


**Fig. 4** (a) 9.77 mmol undischarged Ne : H<sub>2</sub> : NH<sub>3</sub> = 400 : 6 : 1 was codeposited at 4.3 K over a period of 231 min with 9.96 mmol Ne that had been passed through a microwave discharge. (b) 13.4 mmol undischarged Ne : H<sub>2</sub> : ND<sub>3</sub> : NH<sub>3</sub> = 400 : 5 : 0.7 : 0.3 was codeposited at 4.3 K over a period of 250 min with 11.1 mmol Ne that had been passed through a microwave discharge. (c) 11.8 mmol undischarged Ne : H<sub>2</sub> : ND<sub>3</sub> = 400 : 5 : 1 was codeposited at 4.3 K over a period of 220 min with 9.63 mmol Ne that had been passed through a microwave discharge. (d) 11.4 mmol undischarged Ne : D<sub>2</sub> : ND<sub>3</sub> = 400 : 5 : 1 was codeposited at 4.3 K over a period of 215 min with 9.30 mmol Ne that had been passed through a microwave discharge.

the order of increasing deuterium enrichment. The traces labeled (a) were obtained for the same sample as that used for Fig. 1(f) and for Fig. 2(a), with no deuterium enrichment. The traces labeled (b) were obtained in an experiment on a Ne : H<sub>2</sub> : ND<sub>3</sub> : NH<sub>3</sub> = 400 : 5 : 0.7 : 0.3 sample, those labeled (c) in a study of a Ne : H<sub>2</sub> : ND<sub>3</sub> = 400 : 5 : 1 sample, and those labeled (d) in a study of a Ne : D<sub>2</sub> : ND<sub>3</sub> sample. The latter

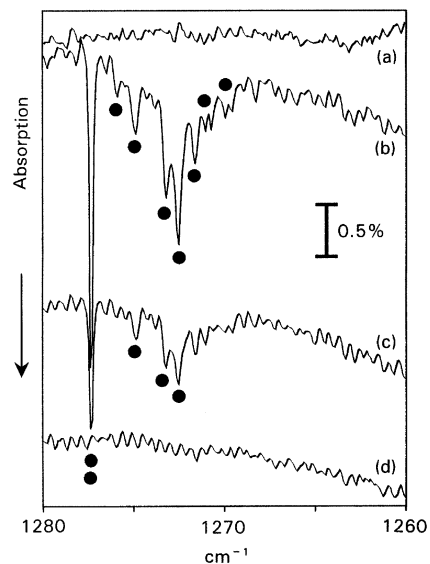


**Fig. 5** (a) 9.77 mmol undischarged Ne : H<sub>2</sub> : NH<sub>3</sub> = 400 : 6 : 1 was codeposited at 4.3 K over a period of 231 min with 9.96 mmol Ne that had been passed through a microwave discharge. (b) 13.4 mmol undischarged Ne : H<sub>2</sub> : ND<sub>3</sub> : NH<sub>3</sub> = 400 : 5 : 0.7 : 0.3 was codeposited at 4.3 K over a period of 250 min with 11.1 mmol Ne that had been passed through a microwave discharge. (c) 11.8 mmol undischarged Ne : H<sub>2</sub> : ND<sub>3</sub> = 400 : 5 : 1 was codeposited at 4.3 K over a period of 220 min with 9.63 mmol Ne that had been passed through a microwave discharge. (d) 11.4 mmol undischarged Ne : D<sub>2</sub> : ND<sub>3</sub> = 400 : 5 : 1 was codeposited at 4.3 K over a period of 215 min with 9.30 mmol Ne that had been passed through a microwave discharge.



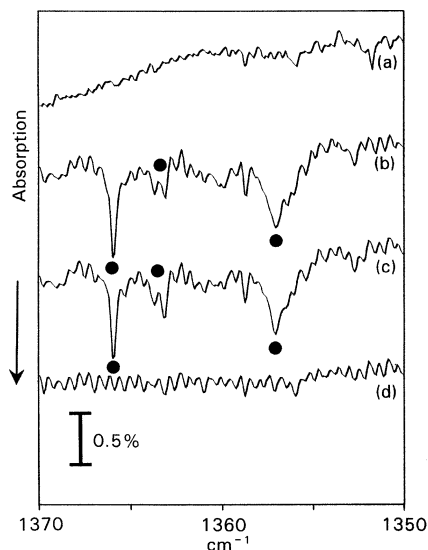


**Fig. 6** (a) 9.77 mmol undischarged Ne : H<sub>2</sub> : NH<sub>3</sub> = 400 : 6 : 1 was codeposited at 4.3 K over a period of 231 min with 9.96 mmol Ne that had been passed through a microwave discharge. (b) 13.4 mmol undischarged Ne : H<sub>2</sub> : ND<sub>3</sub> : NH<sub>3</sub> = 400 : 5 : 0.7 : 0.3 was codeposited at 4.3 K over a period of 250 min with 11.1 mmol Ne that had been passed through a microwave discharge. (c) 11.8 mmol undischarged Ne : H<sub>2</sub> : ND<sub>3</sub> = 400 : 5 : 1 was codeposited at 4.3 K over a period of 220 min with 9.63 mmol Ne that had been passed through a microwave discharge. (d) 11.4 mmol undischarged Ne : D<sub>2</sub> : ND<sub>3</sub> = 400 : 5 : 1 was codeposited at 4.3 K over a period of 215 min with 9.30 mmol Ne that had been passed through a microwave discharge.

sample achieved the highest extent of deuterium enrichment attained in this series of experiments.

As is shown in Fig. 3(d), highly structured, photosensitive absorption appeared between 1085 and 1097 cm<sup>-1</sup>. The strongest absorption maximum was at 1092.0 cm<sup>-1</sup>, but absorptions at 1093.6 and 1093.1 cm<sup>-1</sup> were only slightly weaker. Other relatively prominent absorptions appeared at 1091.6, 1089.7, 1088.3 and 1086.8 cm<sup>-1</sup>. The 1092.0 cm<sup>-1</sup> absorption and its

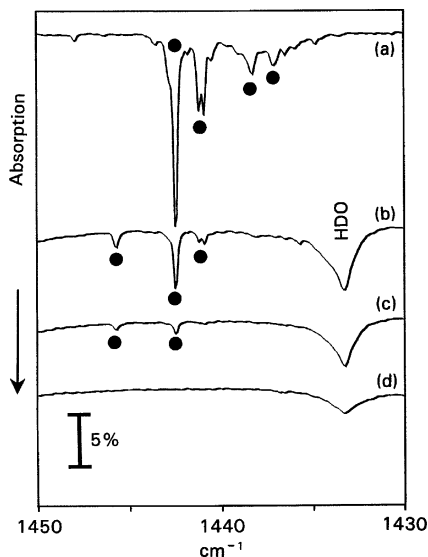


**Fig. 7** (a) 9.77 mmol undischarged Ne : H<sub>2</sub> : NH<sub>3</sub> = 400 : 6 : 1 was codeposited at 4.3 K over a period of 231 min with 9.96 mmol Ne that had been passed through a microwave discharge. (b) 13.4 mmol undischarged Ne : H<sub>2</sub> : ND<sub>3</sub> : NH<sub>3</sub> = 400 : 5 : 0.7 : 0.3 was codeposited at 4.3 K over a period of 250 min with 11.1 mmol Ne that had been passed through a microwave discharge. (c) 11.8 mmol undischarged Ne : H<sub>2</sub> : ND<sub>3</sub> = 400 : 5 : 1 was codeposited at 4.3 K over a period of 220 min with 9.63 mmol Ne that had been passed through a microwave discharge. (d) 11.4 mmol undischarged Ne : D<sub>2</sub> : ND<sub>3</sub> = 400 : 5 : 1 was codeposited at 4.3 K over a period of 215 min with 9.30 mmol Ne that had been passed through a microwave discharge.

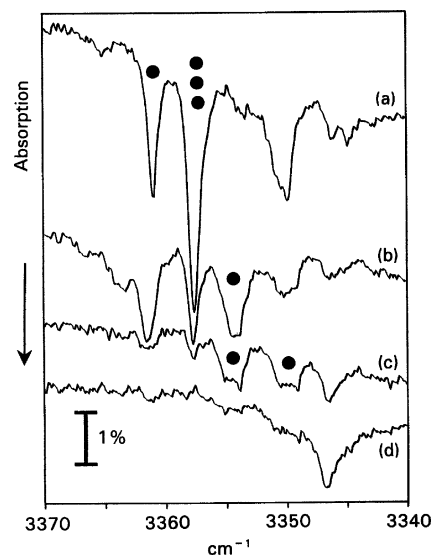


**Fig. 8** (a) 9.77 mmol undischarged Ne : H<sub>2</sub> : NH<sub>3</sub> = 400 : 6 : 1 was codeposited at 4.3 K over a period of 231 min with 9.96 mmol Ne that had been passed through a microwave discharge. (b) 13.4 mmol undischarged Ne : H<sub>2</sub> : ND<sub>3</sub> : NH<sub>3</sub> = 400 : 5 : 0.7 : 0.3 was codeposited at 4.3 K over a period of 250 min with 11.1 mmol Ne that had been passed through a microwave discharge. (c) 11.8 mmol undischarged Ne : H<sub>2</sub> : ND<sub>3</sub> = 400 : 5 : 1 was codeposited at 4.3 K over a period of 220 min with 9.63 mmol Ne that had been passed through a microwave discharge. (d) 11.4 mmol undischarged Ne : D<sub>2</sub> : ND<sub>3</sub> = 400 : 5 : 1 was codeposited at 4.3 K over a period of 215 min with 9.30 mmol Ne that had been passed through a microwave discharge.

satellites lie close to the 1094.9 cm<sup>-1</sup> position calculated for the previously unreported  $\nu_4$  fundamental of ND<sub>4</sub><sup>+</sup>. (Here and in the following discussion, all of the calculated positions for isotopomers of the ammonium cation – summarized in Table 1 – are those obtained in the study by Martin and Lee.<sup>9</sup>) The photosensitive absorption at 1103.4 cm<sup>-1</sup>, most prominent in traces (b) and (c) of Fig. 3, also lies close to the absorption of NHD<sub>3</sub><sup>+</sup> which is calculated to appear at 1101.0 cm<sup>-1</sup>. Photosensitive absorptions at 1099.6 and 1094.6 cm<sup>-1</sup> may possibly be contributed by the same fundamental of NHD<sub>3</sub><sup>+</sup>.

In the 1130 to 1150 cm<sup>-1</sup> spectral region, shown in Fig. 4, a sharp, photosensitive absorption appeared at 1139.9 cm<sup>-1</sup> in the experiments with a moderate extent of deuterium enrichment. This peak was accompanied by less well defined, photosensitive peaks at 1133.5 and 1131.6 cm<sup>-1</sup>. The correlation of the 1139.9 cm<sup>-1</sup> peak with the 1140.6 cm<sup>-1</sup> peak calculated for NHD<sub>3</sub><sup>+</sup> is evident.

The 1260 to 1280 cm<sup>-1</sup> spectral region is shown for these four samples in Fig. 5, which may be compared to the related observations for samples prepared using HD or D<sub>2</sub> illustrated in Fig. 2. In the experiments of Fig. 5(b) and 5(c), as in those of Fig. 2(b) and 2(c), the most prominent photosensitive product absorption appears at 1277.3 cm<sup>-1</sup>, very close to the 1278.6 cm<sup>-1</sup> position calculated for one of the vibrational fundamentals of NH<sub>3</sub>D<sup>+</sup>. Within the experimental error, the most prominent satellite absorptions, at 1273.2 and 1272.5 cm<sup>-1</sup>, correspond with relatively prominent peaks in the experiment of Fig. 2(c).

As is shown in Fig. 6, a sharp, photosensitive absorption appears at 1365.9 cm<sup>-1</sup> in the spectrum of samples with an intermediate extent of deuterium substitution. This peak corresponds well with the most intense deformation fundamental of NH<sub>2</sub>D<sub>2</sub><sup>+</sup>, calculated to appear at 1363.5 cm<sup>-1</sup>. Satellite absorptions also appear at 1363.4 and 1357.0 cm<sup>-1</sup>.

The 1430 to 1450 cm<sup>-1</sup> spectral region is shown for this set of samples in Fig. 7. The photosensitive absorption at 1442.5 cm<sup>-1</sup> and its less intense companions at 1441.2 and 1440.9 cm<sup>-1</sup> decrease rapidly in intensity as the extent of deuterium substitution of the sample grows. A weak, photosensitive

absorption appears at  $1447.9\text{ cm}^{-1}$ . Possibly this absorption is contributed by a deformation vibration of  $\text{NH}_3\text{D}^+$ , detectable at the concentration of  $\text{NH}_3\text{D}^+$  achieved in the experiments shown in Fig. 7(b) and 7(c) but not in the experiments of Fig. 2(b) and 2(c). However, this identification is tentative. In the experiments of Fig. 7(b) and 7(c), a weak, sharp, photosensitive absorption also appeared at  $1425.0\text{ cm}^{-1}$ , close to the  $1426.9\text{ cm}^{-1}$  position calculated for a deformation fundamental of  $\text{NHD}_3^+$ .

The  $2500\text{ cm}^{-1}$  spectral region, characteristic of the ND-stretching vibrations of both uncharged deuterium-substituted ammonia and the fully and partially deuterium substituted ammonium cation, shows a very complicated absorption spectrum. The most prominent photosensitive peak in the highest deuterium enrichment study lies at  $2502.1\text{ cm}^{-1}$ , in good agreement with the calculated position of  $2492.0\text{ cm}^{-1}$  and the gas-phase band center<sup>2</sup> observed at  $2495.0\text{ cm}^{-1}$  for  $\nu_3$  of  $\text{ND}_4^+$ .

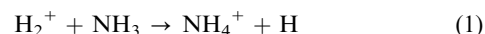
The  $3340$  to  $3370\text{ cm}^{-1}$  absorption region, shown in Fig. 8, includes several NH-stretching absorptions of  $\text{NH}_4^+$  and its partially deuterium-substituted isotopomers. In trace (a), the most prominent absorption is the photosensitive peak at  $3357.5\text{ cm}^{-1}$ , which has a less intense companion at  $3361.0\text{ cm}^{-1}$ . The major peak acquires a lower frequency counterpart at  $3354.2\text{ cm}^{-1}$  when some deuterium is introduced into the ammonia molecule, as in traces (b) and (c). The assignment of that absorption to  $\text{NH}_3\text{D}^+$  is consistent with the calculations and with the identification<sup>8</sup> of the gas-phase band center of  $\nu_4$  of  $\text{NH}_3\text{D}^+$  at  $3341.08\text{ cm}^{-1}$ ,  $2.06\text{ cm}^{-1}$  below the position of the  $\text{NH}_4^+$  stretching absorption. Although the peak at  $3350.0\text{ cm}^{-1}$  did not decrease on mercury-arc irradiation of the deposits of traces (a) and (b), it did decrease in the experiment of trace (c), suggesting that in the latter experiment much or all of the absorption at that frequency arises from  $\text{NH}_2\text{D}_2^+$ . In the experiments of traces (b) and (c), a photosensitive absorption (not shown in Fig. 8) also appeared at  $3306.4\text{ cm}^{-1}$ , a position appropriate for its assignment to the second NH-stretching fundamental of  $\text{NH}_2\text{D}_2^+$ .

Experiments were also conducted on samples prepared using  $^{15}\text{NH}_3$  and  $^{15}\text{ND}_3$ . The results were analogous to those already described, except that each of the absorptions is shifted to a slightly lower frequency. In Table 2, the observed shifts are compared with those obtained from RMP2/6-311++G(3df,3pd) calculations. To correct for anharmonicity, each vibration calculated for the nitrogen-15 substituted cation was scaled by a factor derived from the ratio of the observed

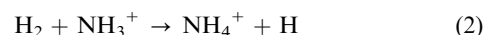
vibrational frequency for the nitrogen-14 substituted species to the corresponding calculated value. None of the observed isotopic shifts deviated from the calculated shift by more than  $0.9\text{ cm}^{-1}$ , providing further support for the proposed assignments.

### C. Processes which occur in the matrix

The results of all of the earlier studies in this laboratory using a beam of pure neon that had been passed through a microwave discharge are consistent with ion production by interaction of a suitable precursor with excited neon atoms and their resonance radiation, in the  $16.6$  to  $16.85\text{ eV}$  energy range. Since those energies, for the first group of excited states of the neon atom, exceed the first ionization energy of both  $\text{NH}_3$  ( $10.17\text{ eV}^{11,24}$ ) and  $\text{H}_2$  ( $15.43\text{ eV}^{25}$ ), the two reactions



and



may both occur in the region between the pinhole in the discharge tube and the cryogenic surface, as well as on the surface itself. However, because of the large disparity between the values of the first ionization energies of  $\text{H}_2$  and  $\text{NH}_3$ , collisional charge exchange between  $\text{H}_2^+$  and  $\text{NH}_3$  is likely to occur. Therefore, Reaction (2) would be likely to predominate.

Early gas phase studies<sup>26,27</sup> determined a relatively slow rate ( $k = 5 \times 10^{-13}\text{ cm}^3\text{ s}^{-1}$ ) rate for Reaction (2) at room temperature. This rate increased as the temperature was raised, permitting estimation of an activation energy of  $8.8\text{ kJ mol}^{-1}$  ( $2.1\text{ kcal mol}^{-1}$ ). When the reaction mixture was cooled, it was found<sup>28,29</sup> that the rate levels off between  $80$  and  $100\text{ K}$ . At lower temperatures, the rate increases again.<sup>30,31</sup> Studies of isotopically enriched samples determined<sup>29,32</sup> that the rate of the reaction between  $\text{D}_2$  and  $\text{NH}_3^+$  is only about  $10\%$  as great as that for  $\text{H}_2$  and  $\text{NH}_3^+$ . Several laboratories<sup>32–35</sup> have also studied the comparative yields of  $\text{NH}_3\text{D}^+$  and  $\text{NH}_2\text{D}^+$  in the  $\text{D}_2 + \text{NH}_3^+$  system for various  $\text{NH}_3^+$  vibrational energies and center-of-mass collision energies. Although  $\text{NH}_3\text{D}^+$  is always the predominant product, at higher collision energies some  $\text{NH}_2\text{D}^+$  is also formed.

Herbst and co-workers<sup>36</sup> obtained good agreement between their calculated rate coefficients and the values derived from the experimental data for a mechanism that postulated the initial formation of a  $\text{NH}_3^+ \cdots \text{H}_2$  complex, bound by  $5.9(1.3)\text{ kJ mol}^{-1}$ , or  $1.4(3)\text{ kcal mol}^{-1}$ , which has a long lifetime at low temperatures and decomposes by tunneling. The exit channel complex,  $\text{NH}_4^+ \cdots \text{H}$ , is bound by less than  $3\text{ kJ mol}^{-1}$  and readily decomposes to form  $\text{NH}_4^+ + \text{H}$ . Their model is consistent with the observed reaction rates for the deuterium-substituted species. Herbst and co-workers also calculated the rates for the three-body reaction (which also involved a helium atom) and found that the results were compatible with other observations.<sup>30</sup> The three-body reaction differs by collisional stabilization of the  $\text{NH}_3^+ \cdots \text{H}_2$  complex, which is found still to be able to undergo tunneling to form the products on a time scale shorter than that of the observations. These conditions are likely to predominate during matrix depositions and in solid neon.

The structure observed for the vibrational fundamentals of the  $\text{NH}_4\text{-}d_n^+$  species may arise in part from the trapping of the molecules in various types of site in the solid neon. Site splittings have been observed for  $\text{NH}_3$ <sup>20,21</sup> and for many other molecules trapped in the solid rare gases. However, other phenomena must be invoked to explain the disparity between the absorption patterns observed for  $\nu_4$  of  $\text{NH}_4^+$  and  $\text{ND}_4^+$ .

The complicated vibrational absorption patterns observed in the present series of experiments might arise from molecular

**Table 2** Nitrogen-15 shifts (in  $\text{cm}^{-1}$ ) for observed absorptions of  $\text{NH}_4\text{-}d_n^+$

Species	$\nu_{\text{obs}}^a$	$\Delta_{\text{obs}}$	$\Delta_{\text{MP2}}^b$
$\text{NH}_4^+$	3357.5	8.4	9.3
	1442.5	6.8	6.8
$\text{NH}_3\text{D}^+$	3354.2	8.6	8.1
	1277.3	6.6	6.7
$\text{NH}_2\text{D}_2^+$	3350.0	9.0	9.3
	1365.9	5.8	6.0
$\text{NHD}_3^+$	1139.9	5.5	5.1
	1103.4	8.4	8.5
$\text{ND}_3^+$	2502.1	12.6	13.4
	1092.0	7.5	7.6

<sup>a</sup> Nitrogen-14 species, Ne matrix, this work. Based on previous investigations, the standard uncertainty (Type B) in the frequency measurement is  $\pm 0.1\text{ cm}^{-1}$  (coverage factor,  $k = 1$ : i.e.,  $1\sigma$ ). <sup>b</sup> From RMP2/6-311++G(3df,3pd) calculations (this work), scaled to match MP2 frequency of  $^{14}\text{NH}_4\text{-}d_n^+$  to observed value.

**Table 3** Comparison of calculated<sup>a</sup> absorptions (in cm<sup>-1</sup>) for selected isotopomers of NH<sub>4</sub><sup>+</sup> and NH<sub>4</sub><sup>+</sup>...H

NH <sub>4</sub> <sup>+</sup>	NH <sub>4</sub> <sup>+</sup> ...H	NH <sub>4</sub> <sup>+</sup> ...D	ND <sub>4</sub> <sup>+</sup>	ND <sub>4</sub> <sup>+</sup> ...H	ND <sub>4</sub> <sup>+</sup> ...D
3538.1(580) f <sub>2</sub>	3539.9(374) e 3497.4(299) a <sub>1</sub>	3539.9(376) e 3497.4(299) a <sub>1</sub>	2607.6(300) f <sub>2</sub>	2608.7(192) e 2576.2(165) a <sub>1</sub>	2608.8(192) e 2576.2(165) a <sub>1</sub>
3402.3(0) a <sub>1</sub>	3384.7(36) a <sub>1</sub>	3384.7(36) a <sub>1</sub>	2406.7(0) a <sub>1</sub>	2396.5(7) a <sub>1</sub>	2396.5(7) a <sub>1</sub>
1741.0(0) e	1742.5(0.6) e	1742.5(0.6) e	1231.5(0) e	1232.6(0.2) e	1232.6(0.2) e
1478.7(417) f <sub>2</sub>	1482.7(244) e 1474.3(132) a <sub>1</sub> 260.7(13) a <sub>1</sub> 147.6(0.1) e	1482.7(244) e 1474.3(132) a <sub>1</sub> 189.2(14) a <sub>1</sub> 140.4(0.01) e	1110.3(153) f <sub>2</sub>	1113.0(88) e 1106.8(46) a <sub>1</sub> 259.4(11) a <sub>1</sub> 114.5(0.04) e	1113.0(88) e 1106.8(46) a <sub>1</sub> 187.4(11) a <sub>1</sub> 104.8(0.1) e

<sup>a</sup> MP2/6-311++G(3df,3pd) calculations, unrestricted for complexes. Infrared intensities (in km mol<sup>-1</sup>) are given in parentheses. The symmetry of NH<sub>4</sub><sup>+</sup> and ND<sub>4</sub><sup>+</sup> is T<sub>d</sub>, but that of the atom-cation complexes is C<sub>3v</sub>.

rotation. Simple uncharged molecular hydrides usually can rotate in a neon matrix. The rotation of ammonia in solid neon has previously been studied.<sup>20,21</sup> High-resolution infrared observations<sup>37</sup> of a very dilute Ne : CH<sub>4</sub> sample suggested that although CH<sub>4</sub>, which is geometrically similar to NH<sub>4</sub><sup>+</sup>, can rotate in argon and the heavier rare-gas matrices, it cannot rotate in solid neon. Beginning with the high-resolution observations by Momose and co-workers,<sup>38</sup> the rotation of CH<sub>4</sub> in solid parahydrogen has been extensively studied. At 4.8 K, the most prominent absorption of each of the two infrared-active vibrational fundamentals of CH<sub>4</sub> is contributed by the R(0) transition. Other components of the rotational structure are symmetrically placed about it, with spacings of approximately 5 cm<sup>-1</sup>. Although, with appropriately smaller spacings, a similar pattern of absorptions is observed for ND<sub>4</sub><sup>+</sup>, the pattern for NH<sub>4</sub><sup>+</sup> is quite different. Whether NH<sub>3</sub><sup>+</sup> and other ions of the simple hydrides can rotate in a neon matrix is not known with certainty. However, there is abundant evidence that the rotation of uncharged hydride molecules is suppressed in the presence of an ion field.<sup>11</sup> Therefore, other explanations for the observed structure must also be considered.

A major contributor to the observed structure is likely to be complexation of NH<sub>4</sub><sup>+</sup> by other species present in the matrix. The interaction energy for the NH<sub>4</sub><sup>+</sup>...NH<sub>3</sub> pair<sup>39</sup> is relatively large, but in the present experiments the probability of collisional interaction between NH<sub>3</sub> and NH<sub>4</sub><sup>+</sup> is much smaller than that between H<sub>2</sub> and NH<sub>4</sub><sup>+</sup>.

At the H<sub>2</sub> concentrations necessary to obtain an appreciable yield of NH<sub>4</sub><sup>+</sup>, the stabilization of that species with one or more nearest neighbor H<sub>2</sub> molecules is highly probable. Calculations by Urban and co-workers<sup>40</sup> indicate that up to eight H<sub>2</sub> molecules can complex with NH<sub>4</sub><sup>+</sup>. The first solvation shell is filled by four H<sub>2</sub> molecules, each oriented with its axis perpendicular to that of the NH bond with which it interacts. At the MP4 level, the solvation energy of each of these four H<sub>2</sub> molecules is approximately 10 kJ mol<sup>-1</sup> (2.4 kcal mol<sup>-1</sup>). When deuterium atoms are introduced into the system, interactions with HD and with D<sub>2</sub> will also occur, resulting in small changes in the infrared absorption pattern. Because of the several possible interactions, the absorption pattern in the deuterium-substitution experiments may become quite complex, as is observed.

The calculations by Herbst and co-workers<sup>36</sup> indicate that the transition state for the reaction between NH<sub>3</sub><sup>+</sup> and H<sub>2</sub> rearranges into a weakly bound NH<sub>4</sub><sup>+</sup>...H complex, raising the possibility that this entrance channel complex may also contribute to the observed spectrum. Some of the H atoms are likely to be formed with sufficient kinetic energy to escape from the site of their production. However, the presence of an abundance of neon atoms will encourage collisional deactivation of the initially formed complex. The results of calculations of the positions of the vibrational fundamentals of NH<sub>4</sub><sup>+</sup> and ND<sub>4</sub><sup>+</sup> complexed with a single H or D atom, performed at the UMP2/6-311++G(3df,3pd) level using the Gaussian 03 pro-

gram package,<sup>41</sup> are summarized in Table 3. The reduction in symmetry from T<sub>d</sub> to C<sub>3v</sub> because of complex formation leads to a splitting of approximately 40 cm<sup>-1</sup> in the infrared-active NH-stretching vibration and 8 cm<sup>-1</sup> in the infrared-active deformation vibration. The magnitudes of these splittings are independent of whether an H atom or a D atom participates in the complex. The calculated splitting of the deformation vibration could explain some of the observed structure. However, a lower frequency component of the NH-stretching fundamental was not identified. Such an absorption may have been obscured by one of the prominent absorptions of the photolytically stable NH<sub>3</sub>... (H<sub>2</sub>)<sub>n</sub> species which appeared in these experiments at 3314, 3319 and 3333 cm<sup>-1</sup>. Therefore, the contribution of infrared absorptions of the exit channel complex to the observed spectrum remains uncertain.

As in the earlier study of the infrared spectrum of NH<sub>3</sub><sup>+</sup>,<sup>11</sup> the identity of the anion(s) which provide for the requisite overall charge neutrality of the sample deposit is not revealed by the present experiments, presumably because these species are weak infrared absorbers. A leading candidate would be NH<sub>2</sub><sup>-</sup>, which is calculated<sup>42</sup> to have its bending vibration fundamental in the same spectral region as that of ν<sub>4</sub> of NH<sub>4</sub><sup>+</sup>. However, the two stretching fundamentals of NH<sub>2</sub><sup>-</sup> are calculated<sup>42,43</sup> to lie between 3100 and 3200 cm<sup>-1</sup> and to be much more strongly infrared absorbing than the bending fundamental. The experimentally determined band centers of these stretching fundamentals lie at 3121.93 and 3190.29 cm<sup>-1</sup>.<sup>44,45</sup> In the present experiments, no new absorptions were detected in that spectral region.

## IV. Conclusions

A considerably higher yield of NH<sub>4</sub><sup>+</sup> is obtained in cryogenic sampling experiments when NH<sub>3</sub> and H<sub>2</sub> are introduced into the system downstream from neon atoms that are excited in a microwave discharge than when either molecule is introduced into the discharge region. Since extensive atomization occurs in discharges, the predominant source of NH<sub>4</sub><sup>+</sup> in these experiments is believed to be the reaction of NH<sub>3</sub><sup>+</sup> with H<sub>2</sub>. The neon-matrix shifts in the infrared-active vibrational fundamentals of NH<sub>4</sub><sup>+</sup> are smaller than 0.5%. These experiments have yielded the first identifications of the ν<sub>4</sub> vibrational fundamental of ND<sub>4</sub><sup>+</sup> and of several of the vibrational fundamentals of each of the partially deuterated ammonium cations. Complexation of H atoms and of H<sub>2</sub> with the NH<sub>4</sub>-d<sub>n</sub><sup>+</sup> is believed to be a major contributor to the satellite absorptions which appear close to each of the fundamental absorptions of the NH<sub>4</sub>-d<sub>n</sub><sup>+</sup> species trapped in the neon matrix.

## References

- 1 M. W. Crofton and T. Oka, *J. Chem. Phys.*, 1983, **79**, 3157–3158.
- 2 M. W. Crofton and T. Oka, *J. Chem. Phys.*, 1987, **86**, 5983–5988.

- 3 E. Schäfer, M. H. Begemann, C. S. Gudeman and R. J. Saykally, *J. Chem. Phys.*, 1983, **79**, 3159–3162.
- 4 E. Schäfer, R. J. Saykally and A. G. Robiette, *J. Chem. Phys.*, 1984, **80**, 3969–3977.
- 5 M. Polak, M. Gruebele, B. W. DeKock and R. J. Saykally, *Mol. Phys.*, 1989, **66**, 1193–1202.
- 6 J. Park, C. Xia, S. Selby and S. C. Foster, *J. Mol. Spectrosc.*, 1996, **179**, 150–158.
- 7 R. Signorell, H. Palm and F. Merkt, *J. Chem. Phys.*, 1997, **106**, 6523–6533.
- 8 T. Nakanaga and T. Amano, *Can. J. Phys.*, 1986, **64**, 1356–1358.
- 9 J. M. L. Martin and T. J. Lee, *Chem. Phys. Lett.*, 1996, **258**, 129–135.
- 10 M. E. Jacox, *Chem. Soc. Rev.*, 2002, **31**, 108–115.
- 11 W. E. Thompson and M. E. Jacox, *J. Chem. Phys.*, 2001, **114**, 4846–4854.
- 12 Certain commercial instruments and materials are identified in this paper in order to specify adequately the experimental procedure. In no case does such identification imply recommendation or endorsement by the National Institute of Standards and Technology, nor does it imply that the instruments or materials identified are necessarily the best available for the purpose.
- 13 M. E. Jacox and W. E. Thompson, *J. Chem. Phys.*, 1989, **91**, 1410–1416.
- 14 D. Forney, W. E. Thompson and M. E. Jacox, *J. Chem. Phys.*, 1992, **97**, 1664–1674.
- 15 M. E. Jacox and W. B. Olson, *J. Chem. Phys.*, 1987, **86**, 3134–3142.
- 16 R. A. Toth, *J. Opt. Soc. Am. B*, 1991, **8**, 2236–2255.
- 17 R. A. Toth, *J. Opt. Soc. Am. B*, 1993, **10**, 2006–2029.
- 18 E. J. Bieske and O. Dopfer, *Chem. Rev.*, 2000, **100**, 3963–3998.
- 19 N. M. Lakin, R. V. Olkhov and O. Dopfer, *Faraday Discuss. Chem. Soc.*, 2001, **118**, 455–476.
- 20 L. Abouaf-Marguin, M. E. Jacox and D. E. Milligan, *J. Mol. Spectrosc.*, 1977, **67**, 34–61.
- 21 M. E. Jacox and W. E. Thompson, *J. Mol. Spectrosc.*, 2004, **228**, 414–431.
- 22 A. Moroz, R. L. Sweany and S. L. Whittenburg, *J. Phys. Chem.*, 1990, **94**, 1352–1357.
- 23 M. J. Frisch, G. W. Trucks, H. B. Schlegel, G. E. Scuseria, M. A. Robb, J. R. Cheeseman, V. G. Zakrzewski, J. A. Montgomery Jr., R. E. Stratmann, J. C. Burant, S. Dapprich, J. M. Millam, A. D. Daniels, K. N. Kudin, M. C. Strain, O. Farkas, J. Tomasi, V. Barone, M. Cossi, R. Cammi, B. Mennucci, C. Pomelli, C. Adamo, S. Clifford, J. Ochterski, G. A. Petersson, P. Y. Ayala, Q. Cui, K. Morokuma, D. K. Malick, A. D. Rabuck, K. Raghavachari, J. B. Foresman, J. Cioslowski, J. V. Ortiz, A. G. Baboul, B. B. Stefanov, G. Liu, A. Liashenko, P. Piskorz, I. Komaromi, R. Gomperts, R. L. Martin, D. J. Fox, T. Keith, M. A. Al-Laham, C. Y. Peng, A. Nanayakkara, C. Gonzalez, M. Challacombe, P. M. W. Gill, B. Johnson, W. Chen, M. W. Wong, J. L. Andres, C. Gonzalez, M. Head-Gordon, E. S. Replogle and J. A. Pople, *GAUSSIAN 98, (Revision A.7)*, Gaussian Inc., Pittsburgh PA, 1998.
- 24 V. H. Dibeler, J. A. Walker and H. M. Rosenstock, *J. Res. Natl. Bur. Stand., Sect. A*, 1966, **70**, 459–493.
- 25 D. Shiner, J. M. Gilligan, B. M. Cook and W. Lichten, *Phys. Rev. A*, 1993, **47**, 4042–4045.
- 26 J. K. Kim, L. P. Theard and W. T. Huntress Jr., *J. Chem. Phys.*, 1975, **62**, 45–52.
- 27 F. C. Fehsenfeld, W. Lindinger, A. L. Schmeltekopf, D. L. Albritton and E. E. Ferguson, *J. Chem. Phys.*, 1975, **62**, 2001–2003.
- 28 D. Smith and N. G. Adams, *Mon. Not. R. Astron. Soc.*, 1981, **197**, 377–384.
- 29 N. G. Adams and D. Smith, *Int. J. Mass Spectrom. Ion Processes*, 1984, **61**, 133–139.
- 30 H. Böhringer, *Chem. Phys. Lett.*, 1985, **122**, 185–189.
- 31 J. A. Luine and G. H. Dunn, *Astrophys. J. Lett.*, 1985, **299**, L67–L70.
- 32 S. E. Barlow and G. H. Dunn, *Int. J. Mass Spectrom. Ion Processes*, 1987, **80**, 227–237.
- 33 P. R. Kemper and M. T. Bowers, *J. Phys. Chem.*, 1986, **90**, 477–481.
- 34 R. J. S. Morrison, W. E. Conaway, T. Ebata and R. N. Zare, *J. Chem. Phys.*, 1986, **84**, 5527–5535.
- 35 J. W. Winniczek, A. L. Braveman, M. H. Shen, S. G. Kelley and J. M. Farrar, *J. Chem. Phys.*, 1987, **86**, 2818–2826.
- 36 E. Herbst, D. J. DeFrees, D. Talbi, F. Pauzat, W. Koch and A. D. McLean, *J. Chem. Phys.*, 1991, **94**, 7842–7849.
- 37 L. H. Jones, S. A. Ekberg and B. I. Swanson, *J. Chem. Phys.*, 1986, **85**, 3203–3210.
- 38 T. Momose, M. Miki, W. Wakabayashi, T. Shida, M.-C. Chan, S. S. Lee and T. Oka, *J. Chem. Phys.*, 1997, **107**, 7707–7716.
- 39 B.-C. Wang, J.-C. Chang, J.-C. Jiang and S.-H. Lin, *Chem. Phys.*, 2002, **276**, 93–106.
- 40 J. Urban, S. Roszak and J. Leszczynski, *Chem. Phys. Lett.*, 2001, **346**, 512–518.
- 41 M. J. Frisch, G. W. Trucks, H. B. Schlegel, G. E. Scuseria, M. A. Robb, J. R. Cheeseman, J. A. Montgomery Jr., T. Vreven, K. N. Kudin, J. C. Burant, J. M. Millam, S. S. Iyengar, J. Tomasi, V. Barone, B. Mennucci, M. Cossi, G. Scalmani, N. Rega, G. A. Petersson, H. Nakatsuji, M. Hada, M. Ehara, K. Toyota, R. Fukuda, J. Hasegawa, M. Ishida, T. Nakajima, Y. Honda, O. Kitao, H. Nakai, M. Klene, X. Li, J. E. Knox, H. P. Hratchian, J. B. Cross, C. Adamo, J. Jaramillo, R. Gomperts, R. E. Stratmann, O. Yazyev, A. J. Austin, R. Cammi, C. Pomelli, J. W. Ochterski, P. Y. Ayala, K. Morokuma, G. A. Voth, P. Salvador, J. J. Dannenberg, V. G. Zakrzewski, S. Dapprich, A. D. Daniels, M. C. Strain, O. Farkas, D. K. Malick, A. D. Rabuck, K. Raghavachari, J. B. Foresman, J. V. Ortiz, Q. Cui, A. G. Baboul, S. Clifford, J. Cioslowski, B. B. Stefanov, G. Liu, A. Liashenko, P. Piskorz, I. Komaromi, R. L. Martin, D. J. Fox, T. Keith, M. A. Al-Laham, C. Y. Peng, A. Nanayakkara, M. Challacombe, P. M. W. Gill, B. Johnson, W. Chen, M. W. Wong, C. Gonzalez and J. A. Pople, *GAUSSIAN 03, (Revision B.01)*, Gaussian Inc., Pittsburgh PA, 2003.
- 42 P. Botschwina, *J. Mol. Spectrosc.*, 1986, **117**, 173–174.
- 43 D. J. Swanton, G. B. Bacskey and N. S. Hush, *Chem. Phys.*, 1986, **107**, 25–31.
- 44 L. M. Tack, N. H. Rosenbaum, J. C. Owrtsky and R. J. Saykally, *J. Chem. Phys.*, 1986, **84**, 7056–7057.
- 45 L. M. Tack, N. H. Rosenbaum, J. C. Owrtsky and R. J. Saykally, *J. Chem. Phys.*, 1986, **85**, 4222–4227.